

In-plane superfluid density and microwave conductivity of the organic superconductor κ -(BEDT-TTF)₂Cu[N(CN)₂]Br: evidence for *d*-wave pairing

S. Milbradt,¹ A. A. Bardin,² C. J. S. Truncik,¹ W. A. Huttema,¹
P. L. Burn,³ S.-C. Lo,³ B. J. Powell,² and D. M. Broun¹

¹*Department of Physics, Simon Fraser University, Burnaby, BC, V5A 1S6, Canada*

²*Centre for Organic Photonics & Electronics, School of Mathematics and Physics,
The University of Queensland, Brisbane, Queensland 4072, Australia*

³*Centre for Organic Photonics & Electronics, School of Chemistry and Molecular Biosciences,
The University of Queensland, Brisbane, Queensland 4072, Australia*

We report measurements of the in-plane microwave surface impedance of a high quality single crystal of the title compound. This yields three independent lines of evidence for *d*-wave pairing: i) a strong, linear temperature dependence of superfluid density; ii) deep in the superconducting state the quasiparticle scattering rate $\Gamma(T) \sim T^3$; and iii) no BCS conductivity coherence peak is observed in the quasiparticle conductivity. The zero-temperature penetration depth, $\lambda_0 = 3220$ Å, is found to be much shorter than in previous reports. We also measure the *in-plane* conductivity above the superconducting critical temperature and use this to test theories of the normal state.

PACS numbers: 74.70.Kn, 74.25.nn, 74.25.fc, 74.25.Bt

It has been widely argued that the doped Mott insulator describes the essential physics of the cuprates [1]. Similarly, the physics of the κ -(ET)₂X salts (ET is an abbreviation of BEDT-TTF) appears to be connected to the bandwidth-controlled Mott transition [2]. Thus, it is essential to identify and understand the important similarities and differences between these two classes of quasi-two-dimensional superconductor. In both the cuprates and the κ -(ET)₂X salts, the superconducting critical temperature is only two orders of magnitude smaller than the Fermi temperature; in this sense, both are high temperature superconductors.

However, while there is a broad consensus that the cuprates are *d*-wave superconductors [3–6], the nature of the pairing state of the κ -(ET)₂X salts remains a contentious issue [7, 8] with the only firm conclusion being that the charge carriers form singlet pairs [9]. This, and the low symmetry of the organics, limits the pairing symmetry to be either *s*-wave or *d*-wave [10], but which is realized is an open question. For example, heat capacity experiments have been used to argue in favour of both *s*-wave [11, 12] and *d*-wave [13] pairing and remain controversial [7]. Measurements of the NMR relaxation rate have also led to conflicting reports of both *s*-wave and unconventional pairing [9]. Disorder studies show a reduction in T_c with increasing scattering [14, 15] but, for larger scattering rates, the suppression of T_c is less than expected for non-*s*-wave superconductors. Measurements of London penetration depth and superfluid density, which directly probe the superconducting quasiparticle spectrum, have also been equivocal. Several studies report data consistent with a nodeless *s*-wave state [16–18]. On the other hand, a particularly high-resolution study found evidence of low energy excitations [19], but obtained an anomalous $T^{3/2}$ temperature dependence of the superfluid density. However, the interpretation of

these experiments was complicated by their inability to measure the *absolute* penetration depth. Critically, no measurement to date has reported the linear temperature dependence of in-plane superfluid density expected for a clean *d*-wave superconductor.

In this Letter we use microwave surface impedance to probe the in-plane charge dynamics of κ -(ET)₂Cu[N(CN)₂]Br, both above and below T_c . In the superconducting state, the experiment measures the *absolute* London penetration depth, λ_L , as a function of temperature. From this we obtain the superfluid density, $\rho_s(T) \equiv 1/\lambda_L^2(T)$. We observe a strong, linear temperature dependence of ρ_s , providing clear evidence of line nodes in the energy gap (if the Fermi surface is fully coherent in three dimensions or point nodes if only a quasi-two dimensional Fermi surface exists), consistent with *d*-wave pairing. The measurements also provide access to the quasiparticle conductivity, σ_1 , from which we extract the quasiparticle scattering rate, Γ , and the *in-plane* normal-state resistivity, $\rho_{||}$. It is important to note that most previous measurements of resistivity in κ -(ET)₂Cu[N(CN)₂]Br have been measured perpendicular to the highly conducting planes due to difficulties in obtaining properly calibrated in-plane resistivity data [20–22]. By providing some of the first reliable measurements of this quantity, the microwave experiment also allows us to perform important tests of dynamical mean field theory (DMFT) [23, 24] and of the predicted Kadowaki–Woods ratio in these materials [25].

Single crystals of κ -(ET)₂Cu[N(CN)₂]Br were grown by controlled electrocrystallization in a dichloromethane solution containing 8% (vol.) ethanol [26]. Low current densities (0.03–0.21 $\mu\text{A}\cdot\text{cm}^{-2}$) and a three-compartment cell were employed to produce high quality single crystals [27]. Crystal growth took ~ 5 weeks and the high quality of the crystals was confirmed by x-ray crystallography.

Measurements of surface impedance, $Z_s = R_s + iX_s$, were carried out at $\omega/2\pi = 19.6$ GHz using the TE_{061} mode of a rutile dielectric resonator. The measurement system was a dilution-refrigerator-based variant of that described in Ref. 28, in which the rutile resonator was mounted inside a superconducting enclosure. A small, platelet single crystal of $\kappa\text{-(ET)}_2\text{Cu[N(CN)}_2\text{]Br}$, measuring $0.5\text{ mm} \times 0.5\text{ mm} \times 0.1\text{ mm}$, was attached to one end of a high-purity silicon rod using a small quantity of vacuum grease. During the experiment it was positioned inside the microwave resonator with the microwave H field applied perpendicular to the conducting layers, to induce in-plane screening currents. The other end of the silicon rod was connected to a temperature-controlled stage *outside* the microwave resonator [29], allowing sample temperature to be varied in the range 0.075 K to 30 K independently of the resonator temperature, which was kept fixed at 1.6 K during the course of the measurements. At the beginning of the experiment, the sample was cooled slowly from room temperature at a maximum rate of 1 K/minute.

Temperature-dependent changes in the sample surface impedance were inferred by cavity perturbation from changes in the resonant frequency, f_0 , and bandwidth, f_B , of the rutile resonator as the temperature of the sample was varied with respect to base temperature: $\Delta R_s + i\Delta X_s = \beta(\Delta f_B/2 - i\Delta f_0)$. Here β is a resonator constant that depends on the geometry of the sample and the spatial structure of the TE_{061} mode. In our experiment β was determined empirically using a PbSn replica sample of known surface resistance. We were not able to measure the residual surface resistance of the sample directly, only $\Delta R_s(T)$, the change with temperature. We will discuss below the implications of this for measurements of the quasiparticle conductivity, but note that uncertainties in residual R_s have no significant effect on our determination of superfluid density. Similarly, the cavity perturbation experiment only directly measures $\Delta X_s(T)$, so we obtain the absolute surface reactance using a normal-state matching technique that works as follows: above T_c , the normal-state microwave conductivity is predominantly real implying $R_s(T) \approx X_s(T)$; this condition is imposed and the absolute reactance determined by adding a *temperature-independent* offset to the $\Delta X_s(T)$ data, as shown in Fig. 1. The $R_s(T)$ and $X_s(T)$ data match very well from T_c to 30 K. This provides an important consistency check, confirming that contributions from thermal expansion and interlayer currents are negligible.

From the surface impedance measurements we obtain the complex conductivity, $\sigma = \sigma_1 - i\sigma_2$, using the local electrodynamic expression $\sigma = i\omega\mu_0/Z_s^2$. This relation applies when electronic length scales such as mean free path, ℓ , and coherence length, ξ , are much less than electromagnetic penetration depths, a limit that is satisfied at all but the lowest temperatures in

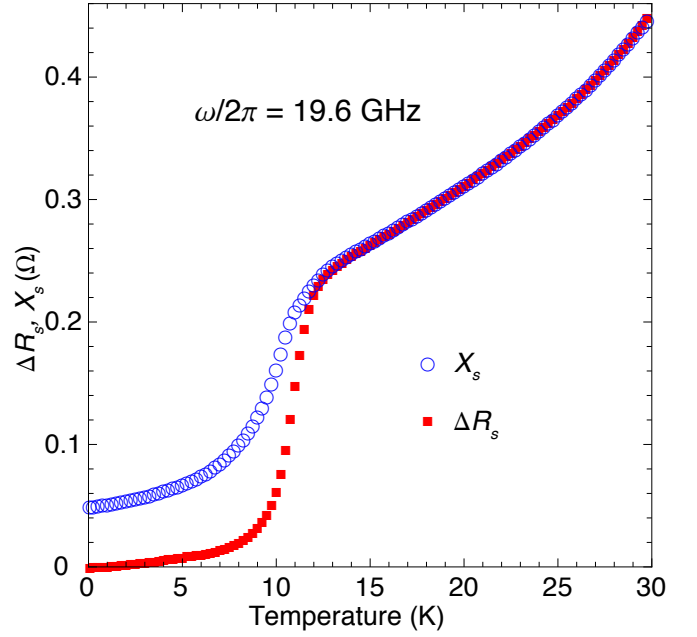


FIG. 1. (color online). Temperature dependence of the 19.6 GHz surface impedance, $Z_s = R_s + iX_s$. The absolute surface reactance is obtained by finding the temperature-dependent offset, X_{s0} , that makes $X_s(T) \equiv X_{s0} + \Delta X_s(T)$ match $R_s(T)$ in the Hagen–Rubens regime above T_c .

$\kappa\text{-(ET)}_2\text{Cu[N(CN)}_2\text{]Br}$ [32]. The superfluid density is obtained from the imaginary part of the conductivity using $\rho_s \equiv 1/\lambda_L^2 = \omega\mu_0\sigma_2$ and is plotted in Fig. 2. We note that our measurement technique, in which we use the normal-state surface impedance as a reference, is able to make an *absolute* determination of X_s . This means that the superfluid density is obtained with very little uncertainty in λ_0 , eliminating spurious curvature that can be present in $\rho_s(T)$ when only $\Delta\lambda(T)$ is measured. As seen in Fig. 2, $\rho_s(T)$ shows a strong, linear temperature dependence over most of the temperature range, similar to that seen in $\text{Ti}_2\text{Ba}_2\text{CuO}_{6+\delta}$ [33] and highly underdoped $\text{YBa}_2\text{Cu}_3\text{O}_{6.333}$ [34]. This is the expected behaviour for an order parameter with line nodes in 3D or point nodes in 2D, and is strong evidence for d -wave pairing symmetry in $\kappa\text{-(ET)}_2\text{Cu[N(CN)}_2\text{]Br}$. At the lowest temperatures there is some slight rounding in $\rho_s(T)$, which we fit using a linear-to-quadratic crossover formula, obtaining a crossover temperature $T_0 = 0.52$ K. While such behaviour is consistent with d -wave superconductivity in the presence of a small density of strong-scattering impurities [35, 36], the inferred value of T_0 is also close to where we expect a crossover to nonlocal electrodynamics in the superfluid density [37], something that is an intrinsic consequence of the nodal structure of a d -wave superconductor and must therefore be present in this temperature range.

From the surface reactance data we obtain a zero temperature penetration depth $\lambda_0 = 3220$ Å, which is

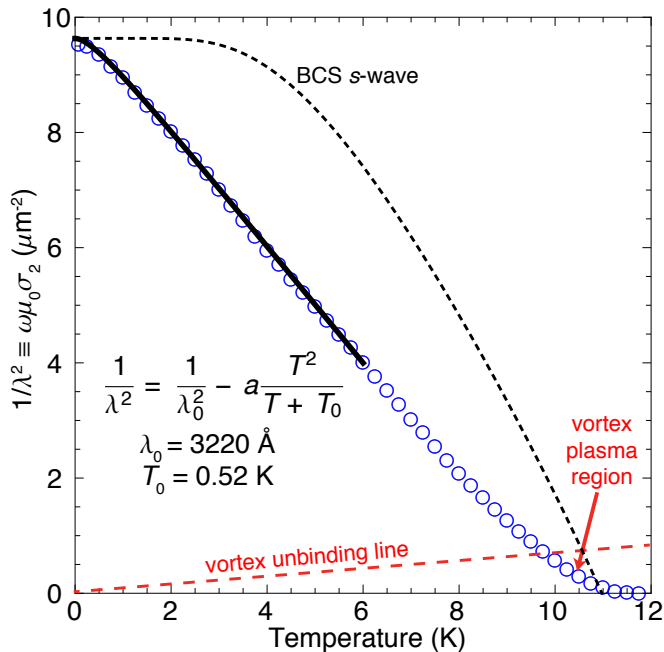


FIG. 2. (color online). Superfluid density, $\rho_s(T) \equiv 1/\lambda_L^2(T) = \omega\mu_0\sigma_2(T)$, obtained from the imaginary part of the microwave conductivity at 19.6 GHz. $\lambda_0 = 3220$ Å is determined from the *absolute* measurement of $X_s(T)$ in Fig. 1, leaving little uncertainty in the shape of $\rho_s(T)$. The superfluid density displays a strong, linear temperature dependence over most of the temperature range, indicating an order parameter with nodes. This is strikingly different from the BCS *s*-wave superfluid density [30] (dashed curve). At very low temperatures $\rho_s(T)$ starts to flatten: the solid line is a fit to a linear-to-quadratic crossover function, $\rho_s(T) = a - bT^2/(T + T_0)$, with cross-over temperature $T_0 = 0.52$ K. The dashed line denotes the expected location of the Kosterlitz–Thouless vortex-unbinding transition. This should occur when the 2D superfluid density $\rho_s^{2D} \equiv \hbar^2 d/4k_B e^2 \mu_0 \lambda_L^2 = (2/\pi)T$, where $d = 15$ Å is the interlayer spacing [31]. $\rho_s(T)$ shows the expected upward curvature close to T_c as it passes through the vortex-plasma regime.

substantially shorter than in earlier studies [17–20, 38–41]. However, we have several reasons to believe that this value is accurate and that superfluid density is actually much higher than previously reported. The microwave data have been calibrated using a replica sample of known surface resistance. This procedure leads to scale errors in surface impedance and penetration depth no larger than 5%, and scale errors in conductivity and superfluid density less than 10%. The reference point for the measurement of absolute penetration depth is the normal-state skin-depth, which at 19.6 GHz is only a factor of 5 larger, therefore leading to relatively small subtraction errors. We emphasize again that the microwave experiment directly measures the *absolute* penetration depth at the same time as it measures the temperature dependence: we obtain $1/\lambda_L^2(T)$ with very little uncertainty in either its shape or magnitude. This leads to the

most important test of our result — comparison with the expected location of the Kosterlitz–Thouless–Berezinskii vortex-unbinding transition [42–45]. This comparison is carried out in Fig. 2, where we show the intersection of $\rho_s(T)$ with the vortex-unbinding line, along which the 2D superfluid density $\rho_s^{2D} \equiv \hbar^2 d/4k_B e^2 \mu_0 \lambda_L^2 = (2/\pi)T$ in each conducting layer. The relatively high value of superfluid density inferred from our measurements means that $\rho_s(T)$ only passes through this regime very close to T_c . We observe some upward curvature of $\rho_s(T)$ in this vicinity, consistent with the superfluid density becoming frequency dependent as the sample enters the vortex-plasma regime, an effect that is prominent in cuprates [46, 47]. If a similar analysis is carried out on previously published data [17–20, 38–41], in which $\rho_s(T)$ is 4 to 40 times smaller, we would expect an abrupt drop in $\rho_s(T)$ somewhere in the range 3 to 8 K. This abrupt drop is not seen in any of the measurements, indicating that the earlier experiments are incompatible with the well-understood vortex-unbinding physics. Finally, we can use the measured value of λ_0 to obtain an estimate of the quasiparticle effective mass, $m^* = ne^2 \mu_0 \lambda_0^2$. Taking $n = 1.21 \times 10^{21}$ cm^{−3} [31], and assuming all electrons condense at low temperature, we obtain $m^* = 4.4m_e$. This is comparable to the cyclotron mass of magnetic breakdown orbits in κ -(ET)₂Cu[N(CN)₂]Br, $m_c = 6.4 \pm 0.5m_e$ [48], and is particularly consistent given the known mass anisotropy around the Fermi surface [49].

The real part of the microwave conductivity is plotted in Supplementary Information in Fig. S1. As mentioned earlier, uncertainties in the residual surface resistance have a substantial effect on the form of $\sigma_1(T)$, but only at low temperatures. To illustrate this, Fig. S1 shows $\sigma_1(T)$ extracted assuming $R_s(T \rightarrow 0) = 0, 2, 4$ and 6 mΩ. The low temperature form of $\sigma_1(T)$ is sensitive to $R_s(T \rightarrow 0)$, but the higher temperature behaviour is largely unaffected. This means that the initial rise in $\sigma_1(T)$ on cooling through T_c is a robust observation and it implies a rapid drop in quasiparticle scattering on entering the superconducting state, which we plot in Fig. 3. Similar behaviour was originally observed in the cuprate superconductors [50, 51] and has subsequently been seen in materials such as the heavy fermion system CeCoIn₅ [52, 53]. The absence of a BCS coherence peak in $\sigma_1(T)$ immediately below T_c provides further confirmation of non-*s*-wave pairing.

To examine the scattering dynamics more closely, we extract the quasiparticle scattering rate, $\Gamma(T)$, using a two-fluid model for the complex conductivity, $\sigma_1 - i\sigma_2 = \epsilon_0 \omega_p^2 [f_s/i\omega + f_n/(i\omega + \Gamma)]$, in which the superfluid and normal fractions satisfy the sum rule $f_s + f_n = 1$ and $\omega_p = c/\lambda_0$ is the plasma frequency [55]. From this, $\Gamma(T) = \omega[\sigma_2(0) - \sigma_2(T)]/\sigma_1(T)$. Note that the expression for Γ is a *ratio* of conductivities, and is therefore insensitive to uncertainties in the resonator constant β . The scattering rate data are plot-

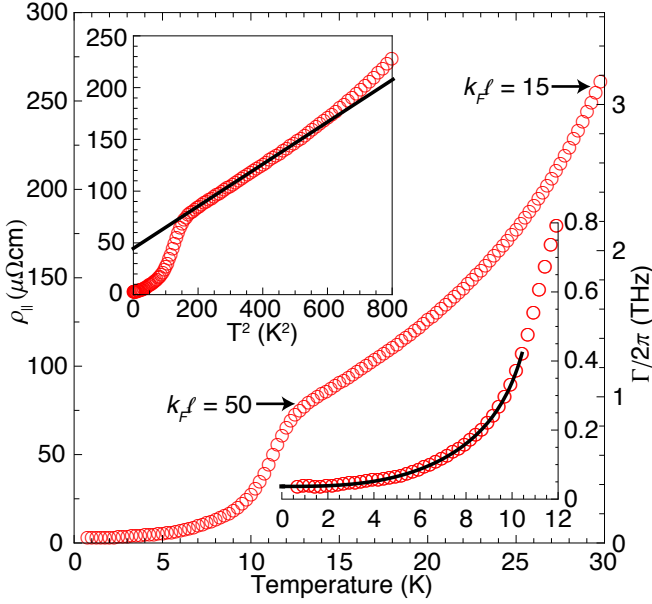


FIG. 3. (color online). In-plane resistivity, $\rho_{||}(T)$, and quasiparticle scattering rate, $\Gamma(T)$. Above T_c , $\rho_{||}(T)$ grows initially as T^2 , steepening with increasing temperature. $k_F\ell \approx 50$ at T_c , falling to 15 by 30 K, where k_F is the Fermi wave vector. Upper inset: $\rho_{||}(T)$ vs. T^2 . Straight line fit is $\rho_{||}(T) = \rho_0 + A_{||}T^2$, with $\rho_0 = 43 \mu\Omega\text{cm}$ and $A_{||} = 0.211 \mu\Omega\text{cm/K}^2$. Lower inset: $\Gamma(T)$ in the superconducting state, fit to $\Gamma(T) = \Gamma_0 + BT^3/\Delta^2(T)$, with $\Gamma_0/2\pi = 47 \text{ GHz}$. $\Delta(T) = \Delta_0(2.7\sqrt{T_c/T} - 1)$ approximates the temperature dependence of the superconducting gap [54].

ted in Fig. 3. At T_c , the scattering rate is several times the thermal energy, similar to the situation in optimally doped cuprates [56] and CeCoIn_5 [52, 53, 57]. On cooling through T_c , $\Gamma(T)$ drops rapidly, indicating that the spectrum of fluctuations responsible for inelastic scattering is of electronic origin, in contrast to the phonon fluctuations of a conventional metal. At lower temperatures, $\Gamma(T) \sim \Gamma_0 + BT^3/\Delta^2$. This behaviour is characteristic of nodal quasiparticles undergoing large-momentum-transfer scattering processes, either due to the exchange of antiferromagnetic spin fluctuations [54, 58], or from direct, short-range repulsion [59, 60]. Interestingly, the energy threshold for exciting Umklapp processes appears to be small [59], suggesting that the gap nodes are separated by approximately a reciprocal lattice vector.

Above T_c , microwave measurements provide a contactless measurement of the in-plane resistivity, $\rho_{||} = 1/\sigma_1$ [20]. Properly calibrated measurements of $\rho_{||}$ are difficult to make by conventional means in the $\kappa\text{-(ET)}_2\text{Cu[N(CN)}_2\text{]Br}$ compounds, due to their large electrical anisotropy [21, 22]. From the new microwave data, a number of key quantities can now be extracted. In addition, we can perform a test of DMFT, which provides a powerful framework for understanding the normal state of organic superconductors [8, 23, 24]. For these materials, DMFT predicts a

Fermi-liquid state immediately above T_c , with a transition to a bad metal, characterized by incoherent charge transport, above a temperature $T^* \approx 50 \text{ K}$. To test this, $\rho_{||}(T)$ is plotted vs. T^2 in the upper inset of Fig. 3, showing that quadratic temperature dependence, a key signature of a Fermi liquid, is indeed observed. The straight-line fit shows $\rho_{||}(T) \approx \rho_0 + A_{||}T^2$, with $\rho_0 = 43 \mu\Omega\text{cm}$ and $A_{||} = 0.211 \mu\Omega\text{cm/K}^2$. The value of the $A_{||}$ coefficient can be compared with a recent prediction of the Kadowaki-Woods ratio in strongly correlated 2D metals [25]:

$$\frac{A_{||}}{\gamma^2} = \frac{81}{4\pi^2\hbar^3 k_B^2 e^2} \frac{n^2}{d}. \quad (1)$$

Here γT is the electronic contribution to the specific heat, n is the electron density, and d is the interlayer spacing. It has been confirmed that this formula is accurate to within a factor of two over a wide range of strongly correlated layered metals [25]. Taking the value of $A_{||}$ reported above, with $n = 1.21 \times 10^{21} \text{ cm}^{-3}$ [31] and $d = 15 \text{ \AA}$ [31], Eq. 1 predicts that $\gamma = 68 \text{ J/m}^3\text{K}^2 = 34 \text{ mJ/mol}\cdot\text{K}^2$. Direct measurements of the heat capacity of $\kappa\text{-(ET)}_2\text{Cu[N(CN)}_2\text{]Br}$ report $\gamma = 22$ to $28 \text{ mJ/mol}\cdot\text{K}^2$ [11, 13, 61], in excellent agreement with the estimate obtained from our measurements and Eq. 1. A key prediction of DMFT is that resistivity reaches the Mott-Ioffe-Regel limit, $k_F\ell = 1$, at T^* . Using the standard expression of resistivity in a 2D metal: $\rho_{||} = \hbar d/e^2 k_F\ell$, we find $k_F\ell \approx 50$ immediately above T_c , decreasing to 15 by 30 K. Extrapolating to higher temperatures, we estimate that $k_F\ell = 1$ for $T \approx 60 \text{ K}$, in accord with the DMFT prediction.

Overall, our measurements give a detailed picture of the behaviour of electrons in $\kappa\text{-(ET)}_2\text{Cu[N(CN)}_2\text{]Br}$. Measurements of the quasiparticle scattering rate allow for key tests of DMFT and the unified theory of the Kadowaki-Woods ratio in this material. The consistency with these theories confirms that the strong electronic correlations central to the normal state of these materials are accurately described by these theories. In the superconducting state we have provided three clear pieces of evidence that d -wave pairing is realised: the linear temperature dependence of the superfluid density; the absence of a BCS conductivity coherence peak; and the T^3 dependence of the quasiparticle scattering rate. The microwave measurements therefore remove the ambiguities arising from previous experiments and finally resolve the question of pairing symmetry in $\kappa\text{-(ET)}_2\text{Cu[N(CN)}_2\text{]Br}$.

The authors thank A. Carrington, R. H. McKenzie and N. C. Murphy for useful discussions/correspondence. Research support was provided by the Natural Science and Engineering Research Council of Canada, the Canadian Foundation for Innovation and the Australian Research Council (projects DP1093224 and DP0878523).

-
- [1] P. A. Lee, N. Nagaosa, and X. G. Wen, *Rev. Mod. Phys.* **78**, 17 (2006).
- [2] B. J. Powell and R. H. McKenzie, *Rep. Prog. Phys.* **74**, 056501 (2011).
- [3] D. J. Scalapino, *Phys. Rep.* **250**, 330 (1995).
- [4] J. F. Annett, N. Goldenfeld, and A. J. Leggett, *J. Low Temp. Phys.* **105**, 473 (1996).
- [5] J. Orenstein and A. J. Millis, *Science* **288**, 468 (2000).
- [6] D. A. Bonn, *Nat. Phys.* **2**, 159 (2006).
- [7] J. Wosnitza, *Crystals* **2**, 248 (2012).
- [8] B. J. Powell and R. H. McKenzie, *J. Phys. Condens. Matter* **18**, R827 (2006).
- [9] K. Miyagawa, K. Kanoda, and A. Kawamoto, *Chem. Rev.* **104**, 5635 (2004).
- [10] B. J. Powell, *J. Phys. Condens. Matter* **18**, L575 (2006).
- [11] H. Elsinger, J. Wosnitza, S. Wanka, J. Hagel, D. Schweitzer, and W. Strunz, *Phys. Rev. Lett.* **84**, 6098 (2000).
- [12] J. Müller, M. Lang, R. Helfrich, F. Steglich, and T. Sasaki, *Phys. Rev. B* **65**, 140509 (2002).
- [13] O. J. Taylor, A. Carrington, and J. A. Schlueter, *Phys. Rev. Lett.* **99**, 057001 (2007).
- [14] J. G. Analytis, A. Ardavan, S. J. Blundell, R. L. Owen, E. F. Garman, C. Jaynes, and B. J. Powell, *Phys. Rev. Lett.* **96**, 177002 (2006).
- [15] T. Sasaki, *Crystals* **2**, 374 (2012).
- [16] M. Lang, N. Toyota, T. Sasaki, and H. Sato, *Phys. Rev. Lett.* **69**, 1443 (1992).
- [17] M. Lang, N. Toyota, T. Sasaki, and H. Sato, *Phys. Rev. B* **46**, 5822 (1992).
- [18] N. Yoneyama, A. Higashihara, T. Sasaki, T. Nojima, and N. Kobayashi, *J. Phys. Soc. Jpn.* **73**, 1290 (2004).
- [19] A. Carrington, I. J. Bonalde, R. Prozorov, R. W. Giannetta, A. M. Kini, J. Schlueter, H. H. Wang, U. Geiser, and J. M. Williams, *Phys. Rev. Lett.* **83**, 4172 (1999).
- [20] M. Dressel, O. Klein, G. Grüner, K. D. Carlson, H. H. Wang, and J. M. Williams, *Phys. Rev. B* **50**, 13603 (1994).
- [21] T. F. Stalcup, J. S. Brooks, and R. C. Haddon, *Phys. Rev. B* **60**, 9309 (1999).
- [22] C. Strack, C. Akinci, V. Pashchenko, B. Wolf, E. Uhrig, W. Assmus, M. Lang, J. Schreuer, L. Wiehl, J. A. Schlueter, J. Wosnitza, D. Schweitzer, J. Müller, and J. Wykhoff, *Phys. Rev. B* **72**, 054511 (2005).
- [23] J. Merino and R. H. McKenzie, *Phys. Rev. B* **61**, 7996 (2000).
- [24] P. Limelette, P. Wzietek, S. Florens, A. Georges, T. A. Costi, C. Pasquier, D. Jerome, C. Meziere, and P. Batail, *Phys. Rev. Lett.* **91**, 016401 (2003).
- [25] A. C. Jacko, J. O. Fjærestad, and B. J. Powell, *Nat. Phys.* **5**, 422 (2009).
- [26] H. Anzai, J. M. Delrieu, S. Takasaki, S. Nakatsuji, and J. Yamada, *J. Cryst. Growth* **154**, 145 (1995).
- [27] A. A. Bardin, P. L. Burn, S. C. Lo, and B. J. Powell, *Phys. Status Solidi B* **249**, 979 (2012).
- [28] W. A. Huttema, B. Morgan, P. J. Turner, W. N. Hardy, X. Zhou, D. A. Bonn, R. Liang, and D. M. Broun, *Rev. Sci. Instrum.* **77**, 023901 (2006).
- [29] S. Sridhar and W. L. Kennedy, *Rev. Sci. Instrum.* **59**, 531 (1988).
- [30] R. Prozorov and R. W. Giannetta, *Supercond. Sci. Tech.* **19**, R41 (2006).
- [31] T. Ishiguro, K. Yamaji, and G. Saito, *Organic superconductors*, 2nd ed. (Springer, 2001).
- [32] The penetration depth is predicted to be affected by nonlocal electrodynamics below a cross-over temperature defined by $k_B T_{nl} \approx (\xi_0/\lambda_0)\Delta_0$ [37]. Assuming a zero-temperature in-plane coherence length $\xi_0 \approx 50 \text{ \AA}$ [7, 62–64], $T_{nl} \approx 0.35 \text{ K}$, close to the measured cross-over temperature T_0 in $\rho_s(T)$.
- [33] D. M. Broun, D. C. Morgan, R. J. Ormeno, S. F. Lee, A. W. Tyler, A. P. Mackenzie, and J. R. Waldram, *Phys. Rev. B* **56**, R11443 (1997).
- [34] D. M. Broun, W. A. Huttema, P. J. Turner, S. Özcan, B. Morgan, R. Liang, W. N. Hardy, and D. A. Bonn, *Phys. Rev. Lett.* **99**, 237003 (2007).
- [35] M. Prohammer and J. P. Carbotte, *Phys. Rev. B* **43**, 5370 (1991).
- [36] P. J. Hirschfeld and N. Goldenfeld, *Phys. Rev. B* **48**, 4219 (1993).
- [37] I. Kosztin and A. J. Leggett, *Phys. Rev. Lett.* **79**, 135 (1997).
- [38] L. P. Le, G. M. Luke, B. J. Sternlieb, W. D. Wu, Y. J. Uemura, J. H. Brewer, T. M. Riseman, C. E. Stronach, G. Saito, H. Yamochi, H. H. Wang, A. M. Kini, K. D. Carlson, and J. M. Williams, *Phys. Rev. Lett.* **68**, 1923 (1992).
- [39] A. Aburto, L. Fruchter, and C. Pasquier, *Physica C* **303**, 185 (1998).
- [40] M. Pinterić, S. Tomić, M. Prester, D. Drobač, O. Milat, K. Maki, D. Schweitzer, I. Heinen, and W. Strunz, *Phys. Rev. B* **61**, 7033 (2000).
- [41] M. Pinterić, S. Tomić, M. Prester, D. Drobač, and K. Maki, *Phys. Rev. B* **66**, 174521 (2002).
- [42] V. L. Berezinskii, *Sov. Phys. JETP* **34**, 610 (1972).
- [43] J. M. Kosterlitz and D. J. Thouless, *J. Phys. C* **6**, 1181 (1973).
- [44] L. B. Ioffe and A. J. Millis, *J. Phys. Chem. Solids* **63**, 2259 (2002).
- [45] I. F. Herbut and M. J. Case, *Phys. Rev. B* **70**, 094516 (2004).
- [46] J. Corson, R. Mallozzi, J. Orenstein, J. N. Eckstein, and I. Bozovic, *Nature* **398**, 221 (1999).
- [47] L. S. Bilbro, R. V. Aguilar, G. Logvenov, O. Pelleg, I. Boović, and N. P. Armitage, *Nat. Phys.* **7**, 298 (2011).
- [48] H. Weiss, M. V. Kartsovnik, W. Biberacher, E. Steep, A. G. M. Jansen, and N. D. Kushch, *Appl. Magn. Reson.* **66**, 202 (1997).
- [49] J. Merino and R. H. McKenzie, *Phys. Rev. B* **62**, 2416 (2000).
- [50] M. C. Nuss, P. M. Mankiewich, M. L. O'Malley, E. H. Westerwick, and P. B. Littlewood, *Phys. Rev. Lett.* **66**, 3305 (1991).
- [51] D. A. Bonn, P. Dosanjh, R. Liang, and W. N. Hardy, *Phys. Rev. Lett.* **68**, 2390 (1992).
- [52] R. J. Ormeno, A. Sibley, C. E. Gough, S. Sebastian, and I. R. Fisher, *Phys. Rev. Lett.* **88**, 047005 (2002).
- [53] C. J. S. Truncik, W. A. Huttema, P. J. Turner, S. Özcan, N. C. Murphy, P. R. Carrière, E. Thewalt, K. J. Morse, A. J. Koenig, J. L. Sarrao, and D. M. Broun, , arXiv:1210.5571.
- [54] D. Duffy, P. J. Hirschfeld, and D. J. Scalapino, *Phys. Rev. B* **64**, 224522 (2001).
- [55] J. R. Waldram, P. Theopistou, A. Porch, and H.-M.

- Cheah, Phys. Rev. B **55**, 3222 (1997).
- [56] C. M. Varma, P. B. Littlewood, S. Schmitt-Rink, E. Abrahams, and A. E. Ruckenstein, Phys. Rev. Lett. **63**, 1996 (1989).
 - [57] C. Petrovic, P. G. Pagliuso, M. F. Hundley, R. Movshovich, J. L. Sarrao, J. D. Thompson, Z. Fisk, and P. Monthoux, J. Phys. Condens. Matter **13**, L337 (2001).
 - [58] S. M. Quinlan, D. J. Scalapino, and N. Bulut, Phys. Rev. B **49**, 1470 (1994).
 - [59] M. B. Walker and M. F. Smith, Phys. Rev. B **61**, 11285 (2000).
 - [60] T. Dahm, P. J. Hirschfeld, D. J. Scalapino, and L. Zhu, Phys. Rev. B **72**, 214512 (2005).
 - [61] B. Andraka, C. S. Jee, J. S. Kim, G. R. Stewart, K. D. Carlson, H. H. Wang, A. V. S. Crouch, A. M. Kini, and J. M. Williams, Solid State Commun. **79**, 57 (1991).
 - [62] W. K. Kwok, U. Welp, K. D. Carlson, G. W. Crabtree, K. G. Vandervoort, H. H. Wang, A. M. Kini, J. M. Williams, D. L. Stupka, L. K. Montgomery, and J. E. Thompson, Phys. Rev. B **42**, 8686 (1990).
 - [63] M. Lang, F. Steglich, N. Toyota, and T. Sasaki, Phys. Rev. B **49**, 15227 (1994).
 - [64] J. Hagel, S. Wanka, D. Beckmann, J. Wosnitza, D. Schweitzer, W. Strunz, and M. Thumfart, Physica C **291**, 213 (1997).

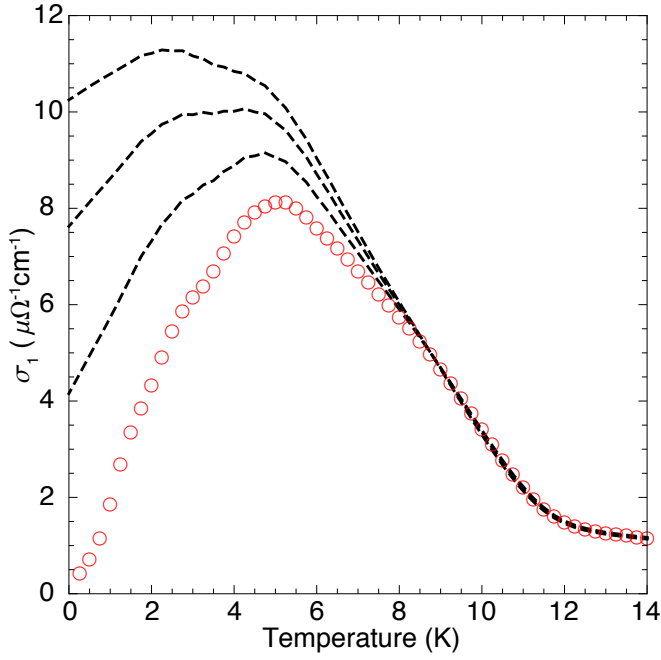


FIG. S1. (color online). Real part of the microwave conductivity, $\sigma_1(T)$, at 19.6 GHz. The lowest trace (open circles) indicates $\sigma_1(T)$ extracted on the assumption that there is no residual surface resistance. The upper traces (dashed lines) show $\sigma_1(T)$ for residual R_s of 2, 4 and 6 m Ω , respectively. The initial rise in $\sigma_1(T)$ on cooling through T_c is robust in the face of uncertainties in residual R_s , and signifies a rapid drop in quasiparticle scattering on entering the superconducting state. Note the absence of a BCS coherence peak below T_c , which would cause $\sigma_1(T)$ to rise almost vertically before falling exponentially at low temperatures.